

## Measurements of an Ablator-Gas Atomic Mix in Indirectly Driven Implosions at the National Ignition Facility

V. A. Smalyuk,<sup>1</sup> R. E. Tipton,<sup>1</sup> J. E. Pino,<sup>1</sup> D. T. Casey,<sup>1</sup> G. P. Grim,<sup>2</sup> B. A. Remington,<sup>1</sup> D. P. Rowley,<sup>1</sup> S. V. Weber,<sup>1</sup> M. Barrios,<sup>1</sup> L. R. Benedetti,<sup>1</sup> D. L. Bleuel,<sup>1</sup> D. K. Bradley,<sup>1</sup> J. A. Caggiano,<sup>1</sup> D. A. Callahan,<sup>1</sup> C. J. Cerjan,<sup>1</sup> D. S. Clark,<sup>1</sup> D. H. Edgell,<sup>3</sup> M. J. Edwards,<sup>1</sup> J. A. Frenje,<sup>4</sup> M. Gatu-Johnson,<sup>4</sup> V. Y. Glebov,<sup>3</sup> S. Glenn,<sup>1</sup> S. W. Haan,<sup>1</sup> A. Hamza,<sup>1</sup> R. Hatarik,<sup>1</sup> W. W. Hsing,<sup>1</sup> N. Izumi,<sup>1</sup> S. Khan,<sup>1</sup> J. D. Kilkenny,<sup>5</sup> J. Kline,<sup>2</sup> J. Knauer,<sup>3</sup> O. L. Landen,<sup>1</sup> T. Ma,<sup>1</sup> J. M. McNaney,<sup>1</sup> M. Mintz,<sup>1</sup> A. Moore,<sup>6</sup> A. Nikroo,<sup>5</sup> A. Pak,<sup>1</sup> T. Parham,<sup>1</sup> R. Petrasso,<sup>4</sup> D. B. Sayre,<sup>1</sup> M. B. Schneider,<sup>1</sup> R. Tommasini,<sup>1</sup> R. P. Town,<sup>1</sup> K. Widmann,<sup>1</sup> D. C. Wilson,<sup>2</sup> and C. B. Yeaman<sup>1</sup>

<sup>1</sup>Lawrence Livermore National Laboratory, Livermore, California 94550, USA

<sup>2</sup>Los Alamos National Laboratory, Los Alamos, New Mexico 87545, USA

<sup>3</sup>Laboratory for Laser Energetics, University of Rochester, Rochester, New York 14623, USA

<sup>4</sup>Massachusetts Institute of Technology, Cambridge, Massachusetts 02139, USA

<sup>5</sup>General Atomics, San Diego, California 92121, USA

<sup>6</sup>AWE Aldermaston, Reading, Berkshire, RG7 4PR, United Kingdom

(Received 14 July 2013; published 14 January 2014)

We present the first results from an experimental campaign to measure the atomic ablator-gas mix in the deceleration phase of gas-filled capsule implosions on the National Ignition Facility. Plastic capsules containing CD layers were filled with tritium gas; as the reactants are initially separated, DT fusion yield provides a direct measure of the atomic mix of ablator into the hot spot gas. Capsules were imploded with x rays generated in hohlraums with peak radiation temperatures of  $\sim 294$  eV. While the TT fusion reaction probes conditions in the central part (core) of the implosion hot spot, the DT reaction probes a mixed region on the outer part of the hot spot near the ablator-hot-spot interface. Experimental data were used to develop and validate the atomic-mix model used in two-dimensional simulations.

DOI: 10.1103/PhysRevLett.112.025002

PACS numbers: 52.57.Fg

The goal of inertial confinement fusion (ICF) [1,2] is to implode a spherical target to achieve high compression of the deuterium-tritium (DT) fuel and high temperature in the hot spot, triggering ignition, and producing significant thermonuclear energy gain. The current indirect-drive ignition point design at the National Ignition Facility (NIF) [3,4] uses a 1.6 MJ laser pulse at a peak power of 410 TW to accelerate the DT fuel to a peak implosion velocity of  $\sim 370$  km/s. The implosion must achieve a temperature of  $T_e > 5$  keV in the central hot spot and high fuel compression with a hot-spot areal density of  $\rho R_{\text{hot-spot}} \sim 0.3$  g/cm<sup>2</sup>, surrounded by a dense main fuel layer with  $\rho R_{\text{fuel}} \sim 1.5$  g/cm<sup>2</sup> to achieve the predicted ignition neutron yield of  $\sim 20$  MJ [5,6]. In recent high-compression experiments on NIF, the fuel areal density of  $\sim 1.3$  g/cm<sup>2</sup> has been achieved with a fuel velocity of  $\sim 320$  km/s. While these two key performance parameters were close to the goal, the neutron yield was reduced by hydrodynamic instabilities and drive asymmetries. As the achieved fuel compression was very close to the requirement, the main focus of the ignition program has shifted towards understanding and mitigating hydrodynamic instabilities and mix, and reducing asymmetries, to increase yield and to enter the alpha-heating (“boot strapping”) regime.

Hydrodynamic instabilities and mix play a central role in performance degradation; any drive asymmetries and

surface imperfections are amplified by hydrodynamic instabilities during the implosion, resulting in a distorted shell with reduced hot-spot temperature, volume, and pressure [3]. In addition, small-scale turbulence seeded by these instabilities can mix ablator material into the DT hot spot. The presence of an ablator-hot-spot mix was correlated with reduced experimental yields and temperatures in high-compression layered DT implosions [5,6], but the nature of this mix (atomic vs “chunk” mix) was unclear. Layered DT implosions have previously been modeled using 2D simulations intended to capture the performance degradation due to instabilities and drive asymmetries [7–9], but lacking a model to predict ablator-fuel atomic mix [7]. While these simulations came close to explaining the DT neutron yields of low-compression implosions (within a factor of 2–3), they were less accurate for ignition-relevant, high-compression implosions, over predicting the yields by a factors from  $\sim 5$  to  $\sim 30$ . Recent 3D simulations improved agreement with experiments slightly, reducing the discrepancy from a factor of  $\sim 5$  to a factor of  $\sim 3$  for one of the best performing shots. As a way to explain the measured performance, 2D simulations used large, unphysical multipliers (up to 3–5 times) on the capsule surface roughness to bring simulated yields down to the measured levels. This raised the possibility that the instability growth factors were larger than in 2D and 3D simulations. Since the

discrepancies were especially pronounced in implosions with significant inferred hot spot mix [10], it was also suggested that the high mode mix at the ablator-hot-spot interface was a major contributor to yield degradation; notably, there were no models of atomic mix used in typical 2D and 3D inertial confinement fusion simulations.

This Letter describes implosion experiments designed to directly measure the signature of an ablator atomic mix, improve the ability to model this mix in 2D simulations [11], and assess the importance of atomic mix to yield degradation. The results presented in our Letter describe a shell-gas atomic mix generated at the inner shell-gas interface by the classical Rayleigh-Taylor (RT) instability [1,2] (with no ablative stabilization) in the deceleration phase of implosions, while previous data (in Refs. [5,6]) were collected in layered DT implosions, where the ablator mix in the DT hot spot was driven at the outer ablation surface by the ablative RT instability in the acceleration phase of implosions. The experiments used capsules with plastic (CH) ablators including deuterated (CD) layers placed at various offsets from the inner surface of the shell. The capsules were filled with high-purity tritium gas to allow the shell-gas atomic mix to be studied using the DT reaction ( $D + T \rightarrow {}^4\text{He} + n$ ) by measuring the DT neutron yield and ion temperature. Variations of this technique were previously used in implosions on OMEGA and NOVA [12–17]. The results presented in this Letter describe the first atomic mix experiments in ignition-relevant conditions with an indirect drive at a moderate convergence ratio of  $\sim 15$  (defined as the ratio of the initial inner-capsule radius to the hot spot radius at peak burn) at NIF. While nuclear observables in our Letter (the DT neutron yield and ion temperature) are solely focused on atomic mix, the x-ray techniques in previous experiments [5,6] were not sensitive to distinguish the atomic mix from other physics including the “chunk” mix. The convergence was chosen to be about 2 times lower than in the layered DT implosions to reduce the high variability of the performance observed in the high-compression implosions that could mask the role of the atomic mix in the performance degradation. We wished to start the investigation of the role of the atomic mix in a region of more predictive simulation capability at a lower convergence. In addition to the DT reactions probing conditions in the mixed region, these experiments also employed TT reactions [18,19] to probe the inner-core region. This significantly constrained the input parameters in the modeling. The results suggest that low-mode ( $l < 100$ ) hydrodynamic instabilities were the primary sources of yield degradation, with the atomic ablator-gas mix playing a secondary role. Based on these results, the ignition program moved toward mitigation of the instability growth and the seeds of these low-mode modulations in the future ignition designs.

Figure 1 shows the capsule schematic and the laser pulse used in these experiments. Plastic shells had a nominal

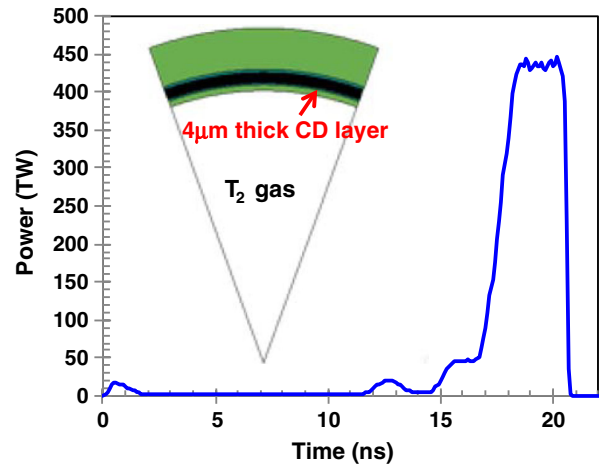


FIG. 1 (color online). Laser pulse shape used in the experiments with a peak power of 436 TW. The inset shows a schematic of the capsule with a nominal outer diameter of 2264  $\mu\text{m}$ , shell thickness of 209  $\mu\text{m}$ , and a 4  $\mu\text{m}$  thick CD layer, placed either at the inner shell surface or recessed from the inner surface by 1.2, 2.3, 3.9, and 8.0  $\mu\text{m}$  of CH layers. The capsules were filled with tritium gas with a mass density of 11.05 mg/cc at a temperature of 32 K.

209  $\mu\text{m}$  thickness and 2280  $\mu\text{m}$ -initial outer diameter [20]. Si-doped layers were included to reduce the preheat of the inner CH ablator from 2–4 keV  $M$ -band emission from the Au hohlraum wall [2]. The capsules for seven implosions included a CD layer with 4.0  $\mu\text{m}$  thickness, placed at either the inner shell surface or offset by 1.2, 2.3, 3.9, and 8.0  $\mu\text{m}$  from the inner surface by a CH-only layer. The shells were filled with tritium gas at a mass density of 11.05 mg/cc and a temperature of 32 K. The tritium gas included an unavoidable small contamination of deuterium gas at a level of 0.1% atom fraction. The background DT yield from this D contamination was measured in two additional implosions that did not contain the CD layers. The DT reactions from these two control implosions were also used as a diagnostic of the central core ion temperature. All implosions used a laser pulse with a peak power of  $\sim 435$  TW and a total laser energy of  $\sim 1.5$  MJ; the same pulse was used in a number of cryogenic layered DT implosions [20]. Details of the laser pulse shape, pointing, and hohlraum geometry were determined in previous experiments as described in Ref. [20]. The capsule and drive parameters were kept very similar in this set of experiments; capsule thickness and outer diameter varied less than 0.5% and 1.5%, respectively, and the laser power profiles were identical to a  $\sim 5\%$  level.

The performance of all implosions was characterized with a comprehensive set of nuclear and x-ray diagnostics [20,21]. The x-ray fluxes of hohlraum radiation from the laser entrance hole were measured with the Dante diagnostic [20]; the inferred x-ray flux temperatures were very repeatable,  $T_r = 294 \pm 4$  eV in all shots. Measured implosion x-ray bang times were  $\sim 22.55 \pm 0.10$  ns, all within 100 ps from each other, with the burn width  $\sim 300$  ps in all

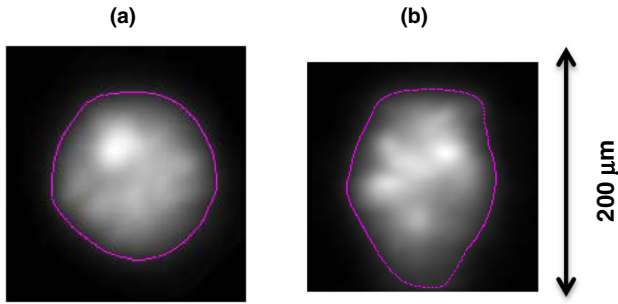


FIG. 2 (color online). Measured time-integrated x-ray images of the imploded core at x-ray photon energies above  $\sim 8$  keV in the (a) polar and (b) equatorial directions. The red curves around the perimeters mark the 17% x-ray intensity contours.

shots. Figure 2 shows examples of the measured x-ray images of the target at bang time in the x-ray range above 8 keV viewed in Fig. 2(a) the polar and in Fig. 2(b) the equatorial directions [22]. The images were good representations of all the implosions, showing nearly round x-ray emission at peak compression. The images show a distinct blotchy structure that is not typical of previous plastic-gas capsule implosions on NIF. The hydrogen gas in our experiments fill radiates less than the He gas fill that is typically used in previous experiments; our images accordingly highlight radiation from the hot higher  $Z$  carbon around the core, accentuating low-mode ( $l \sim 10$ ) shell nonuniformities, discussed below. The 17% contours (relative to peak x-ray brightness) in both polar and equatorial directions had radii of  $\sim 60 \mu\text{m}$ , varying less than 10% from shot to shot. The x-ray shapes of all shots were close to round, with Legendre mode  $P_2/P_0 < \sim 0.1$  (slightly prolate). The measured convergence ratio was about  $\sim 15$ .

Figure 3 shows examples of the measured neutron spectra in implosions with and without CD layers. The

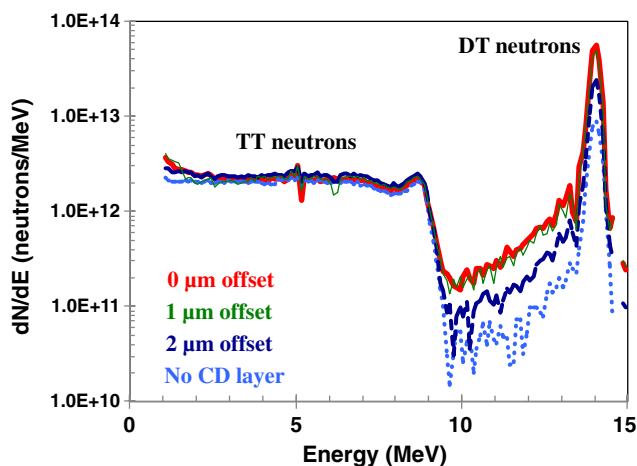


FIG. 3 (color online). Examples of measured neutron spectra with the  $4 \mu\text{m}$  CD layer recessed by  $0 \mu\text{m}$  (thick solid red curve),  $1.18 \mu\text{m}$  (thin solid green curve),  $2.27 \mu\text{m}$  (thick solid blue curve), and without a CD layer (dotted blue curve).

peak at 14.1 MeV was used to measure both the total DT neutron yield and the ion temperature in the DT producing region, while the neutrons below 9 MeV were used to measure TT yield in the central hot spot. Target compression was inferred using the down-scattered ratio (DSR  $\sim 1.2\%$ ) of scattered neutrons in the range from 10 to 12 MeV, relative to the primary neutrons in the range from 13 to 15 MeV [23]. Simulations indicate that roughly half of the down-scattered neutrons were scattered in the tritium gas, while the other half were scattered by the plastic shell [3]. The experimental results were compared with 2D simulations using the code ARES [24]. As direct numerical simulations of the hydrodynamic instabilities including the turbulent mix were not possible, an approximate approach was followed. To capture large wavelength low-mode ( $l < \sim 100$ ) instabilities, simulations were performed using an angular resolution of  $1/8$  degree, with imposed surface roughness at unstable interfaces. The  $K$ - $L$  mix model (where  $K$  represents turbulent kinetic energy, and  $L$  is the spatial scale of the mixing layer) [11] was included to capture the turbulent regime and the effects of mix at scales smaller than the computational grid. The free parameter in this method was the initial turbulent mixing length,  $L_o$ , set at all unstable interfaces.

To calibrate the simulations, a multiplier on the outer ablator surface roughness amplitude was varied. A multiplier of 3 times a nominal value based on the DT capsule specifications was needed to match the measured conditions in the central core, as determined by the TT yield in the capsules with the CD layers directly against the gas. The DT mix yield was then found to match when using a value of  $L_o = 0.1 \text{ nm}$ . The TT yield and core ion temperature were relatively insensitive to the choice of the initial  $L_o$ , suggesting that the local atomic mix near the shell-gas interface does not play a large role in the core performance of these low convergence ratio implosions. These model parameters were then held fixed for the simulations of capsules with recessed CD layers as well as the CH control capsules. Figure 4 shows examples of the 2D ARES simulations of the product of the D and T number densities,  $n_D n_T$ , at a peak burn for implosions with a nonrecessed CD layer (upper half) and a  $\sim 2 \mu\text{m}$  recessed CD layer (lower half). This product is proportional to the DT reactivity at the burn time, and shows the atomically mixed region where 14 MeV neutrons originate. Figure 5 shows the measured neutron results and comparisons with the ARES simulations. The TT yields, DT ion temperatures, DT yields, and ratios of DT/TT yields are shown in Figs. 5(a), 5(b), 5(c), and 5(d), respectively. In implosions without CD layers (labeled “CH capsules”), the measured TT and DT yields along with the DT ion temperatures probed the same conditions in the central part of the core. In implosions with CD layers, the TT yields were similar to those in the CH capsules, while DT yields were up to  $\sim 6$  times higher, and DT ion temperatures were lower ( $\sim 2.0 \text{ keV}$  vs  $3.4 \text{ keV}$ ). The lower measured temperature supports the hypothesis that the DT neutrons

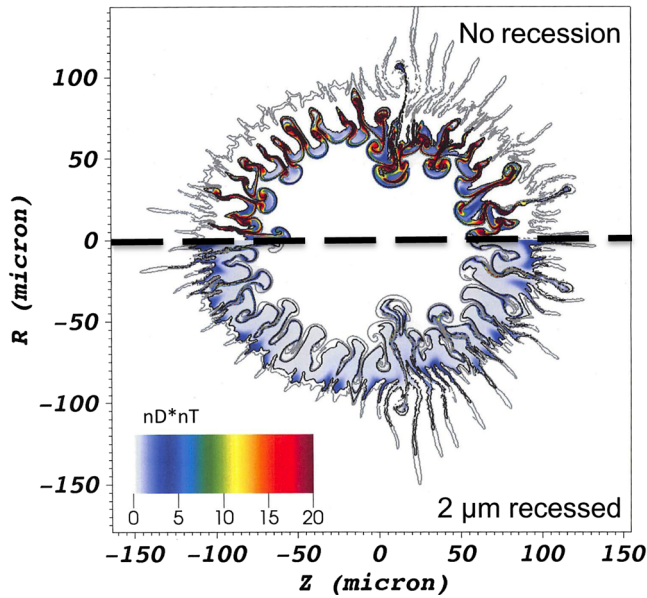


FIG. 4 (color online). The product of the deuterium and tritium number densities, ( $n_D$ ) ( $n_T$ ), for simulations with  $0 \mu\text{m}$  recessed (upper half) and  $2.27 \mu\text{m}$  recessed (bottom half) layers, showing the spatial distribution of the shell-gas mix at this interface. The color scale gives the product,  $n_D n_T$ , in arbitrary units.

were primarily generated in the colder region near the shell-gas interface where D and T were atomically mixed. As the recession of the CD layers from the inner surface increased, the measured DT yields and DT/TT ratios decreased,

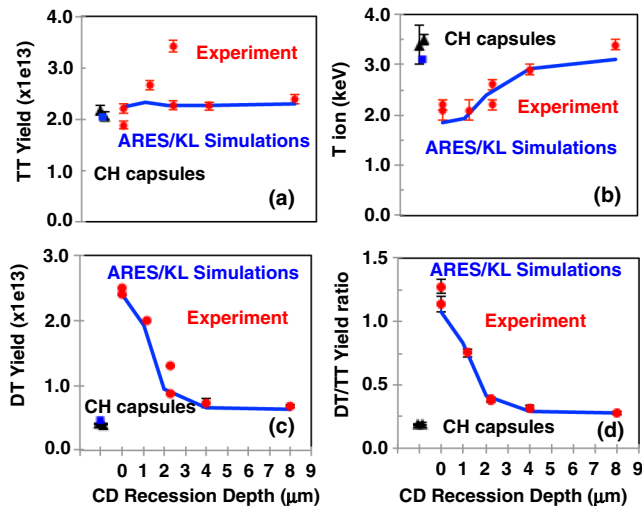


FIG. 5 (color online). Measured and simulated (a) TT neutron yield, (b) the ion temperature inferred from the time-of-flight broadening of the DT fusion yields, (c) DT neutron yield, and (d) the ratio of DT over TT yield as a function of recession depth of the CD layer and for CH capsules without a CD layer. Results of 2D ARES simulations including a  $K$ - $L$  mix model are shown by a solid curve. The blue squares represent simulations of the CH capsules. The experimental measurements are shown by the solid red circles.

indicating that much of the plastic mixed into the gas came from a region close to the inner surface. At the  $2 \mu\text{m}$  recession depth, one of the shots had a  $\sim 40\%$  larger TT yield, compared to all others, due to shot-to-shot performance variability. However, the DT/TT ratio (a primary measure of the atomic mix) was similar to the other shot at the same  $2 \mu\text{m}$  recession. The  $K$ - $L$  model was adjusted to match the DT yield of the nonrecessed capsules but also matches the DT yield and ion temperatures of the recessed capsules quite well.

This need for a large surface roughness multiplier is consistent with previous 2D simulations of high-compression layered DT implosions, which require comparable surface roughness multipliers to match the experimentally measured yields [7]. There are several possible explanations for needing a large multiplier. The effective roughness could in fact be larger than assumed based on current metrology methods. The Rayleigh-Taylor growth rates during the acceleration phase or the preacceleration amplitudes established during the Richtmyer-Meshkov instability phase could be larger than simulated [3]. Some seeds to the instability growth, including radiation asymmetry, shock and release induced chemistry, dust grains and other localized defects, and the effect of the membrane (“tent”) used to support the capsule [25] are not included in the simulations discussed here. To study these processes, measurements of an ablation-front RT growth of preimposed perturbations using x-ray radiography are currently underway at NIF.

In conclusion, an ablator-gas mix was directly studied for the first time at the NIF using DT fusion reactions in implosions with tritium gas filled plastic capsules with localized CD layers in the ablator. Experimental data are consistent with a picture in simulations showing an inner, unmixed core with an ion temperature of  $\sim 3.4 \text{ keV}$  surrounded by a colder mixed region with an ion temperature of  $\sim 2.0 \text{ keV}$ . The 2D simulations (including a  $K$ - $L$  mix model) need 2–6 times increased levels of the surface roughness for the modes below  $1 \sim 100$  to match the measured conditions in the central part of the core. The absolute DT mix yields are sensitive to the  $L_0$  initialization of the mix model, and the simulated mix remains localized to the ablator-gas interface region. The insensitivity of core performance to the mix model suggests that the low-mode hydrodynamic instabilities are the primary cause of yield degradation in cryogenic DT layered implosions, with atomic ablator-gas mix playing a secondary role.

This work was performed under the auspices of the U.S. Department of Energy by Lawrence Livermore National Laboratory under Contract No. DE-AC52-07NA27344.

- [1] S. Atzeni and J. Meyer-ter-Vehn, *The Physics of Inertial Fusion: Beam Plasma Interaction, Hydrodynamics, Hot Dense Matter*, International Series of Monographs on Physics (Clarendon Press, Oxford, 2004).

- [2] J. D. Lindl, *Inertial Confinement Fusion: The Quest for Ignition and Energy Gain Using Indirect Drive* (Springer-Verlag, New York, 1998).
- [3] S. W. Haan *et al.*, *Phys. Plasmas* **18**, 051001 (2011).
- [4] E. I. Moses, R. N. Boyd, B. A. Remington, C. J. Keane, and R. Al-Ayat, *Phys. Plasmas* **16**, 041006 (2009); G. H. Miller, E. I. Moses, and C. R. Wuest, *Opt. Eng.* **443**, 2841 (2004).
- [5] S. P. Regan *et al.*, *Phys. Plasmas* **19**, 056307 (2012).
- [6] T. Ma *et al.*, *Phys. Rev. Lett.* **111**, 085004 (2013).
- [7] D. S. Clark *et al.*, *Phys. Plasmas* **20**, 056318 (2013).
- [8] O. S. Jones *et al.*, *Phys. Plasmas* **19**, 056315 (2012).
- [9] B. K. Spears *et al.*, *Phys. Plasmas* **19**, 056316 (2012).
- [10] V. A. Smalyuk *et al.*, *Phys. Rev. Lett.* **111**, 215001 (2013).
- [11] G. Dimonte and R. Tipton, *Phys. Fluids* **18**, 085101 (2006).
- [12] D. C. Wilson, P. S. Ebey, T. C. Sangster, W. T. Shmayda, V. Yu. Glebov, and R. A. Lerche, *Phys. Plasmas* **18**, 112707 (2011).
- [13] D. D. Meyerhofer *et al.*, *Phys. Plasmas* **8**, 2251 (2001).
- [14] P. B. Radha *et al.*, *Phys. Plasmas* **9**, 2208 (2002).
- [15] C. K. Li *et al.*, *Phys. Rev. Lett.* **89**, 165002 (2002).
- [16] J. Rygg, J. Frenje, C. Li, F. Séguin, R. Petrasso, V. Glebov, D. Meyerhofer, T. Sangster, and C. Stoeckl, *Phys. Rev. Lett.* **98**, 215002 (2007).
- [17] R. E. Chrien, N. M. Hoffman, J. D. Colvin, C. J. Keane, O. L. Landen, and B. A. Hammel, *Phys. Plasmas* **5**, 768 (1998).
- [18] D. T. Casey *et al.*, *Phys. Rev. Lett.* **109**, 025003 (2012).
- [19] D. B. Sayre *et al.*, *Phys. Rev. Lett.* **111**, 052501 (2013).
- [20] S. H. Glenzer *et al.*, *Phys. Plasmas* **19**, 056318 (2012).
- [21] M. J. Edwards *et al.*, *Phys. Plasmas* **18**, 051003 (2011).
- [22] S. Glenn *et al.*, *Rev. Sci. Instrum.* **81**, 10E539 (2010).
- [23] J. A. Frenje *et al.*, *Rev. Sci. Instrum.* **79**, 10E502 (2008).
- [24] R. M. Darlington, T. L. McAbee, and G. Rodrigue, *Comput. Phys. Commun.* **135**, 58 (2001).
- [25] S. W. Haan *et al.*, *Fusion Sci. Technol.* **63**, 67 (2013).